3D Reconstruction with Mirrors and RGB-D Cameras

Abdullah Akay and Yusuf Sinan Akgul
GIT Vision Lab, http://vision.gyte.edu.tr/, Department of Computer Engineering,
Gebze Institute of Technology, 41400, Kocaeli, Turkey
{akay, akgul}@bilmuh.gyte.edu.tr

Keywords: Virtual Cameras, RGB-D Cameras, Kinect, 3D Reconstruction, Multi-view Geometry, Mirrors

Abstract: RGB-D cameras such as Microsoft's Kinect have found many application areas in robotics, 3D modelling and indoor vision due to their low-costs and ease of use. 3D reconstruction with RGB-D cameras is relatively more convenient because they provide RGB and depth data simultaneously for each image element. However, for a full 3D reconstruction of a scene, a single fixed RGB-D camera is inadequate and using multiple cameras brings many challenges with them, such as bandwidth limitations and synchronization. To overcome these difficulties, we propose a solution that employs mirrors to introduce virtual RGB-D cameras into the system. The proposed system does not have any space limitations, data bandwidth constraints, synchronization problems and it is cheaper because we do not require extra cameras. We develop formulations for the simultaneous calibration of real and virtual RGB and RGB-D cameras and we also provide methods for 3D reconstruction from these cameras. We conduct several experiments to assess our system; numerical and visual results are found satisfying.

1 INTRODUCTION

RGB-D cameras such as Microsoft's Kinect sensor have recently found many application areas in robotics, 3D modelling and indoor vision due to their low costs and ease of use. Specifically, these cameras make the 3D reconstruction of objects more convenient because they provide RGB and depth data for each image element simultaneously without any further process. As RGB-D cameras became more reachable, many studies started to appear (Smisek et al., 2013; Henry et al., 2012; Khoshelham et al., 2012) that reconstruct 3D models to be used by ordinary users. Public software libraries (Izadi et al., 2011; Rusu et al., 2011) are now offered to build custom 3D reconstruction software from RGB-D data.

In spite of their convenience, for some cases, a single view of an RGB-D camera is not sufficient to capture the whole 3D scene at the same time for a full reconstruction (Izadi et al., 2011; Henry et al., 2012; Canessa et al., 2013; Oliver et al., 2012). With a single depth map from a fixed RGB-D camera, only visible surfaces can be reconstructed which is inadequate for many applications. One can utilize multiple RGB-D cameras to capture the scene from several viewing locations so that almost all scene surfaces are visible to RGB-D cameras, hence a full 3D reconstruction is possible (Henry et al., 2012; Canessa et al., 2013; Oliver et al., 2012; Lai et al., 2011).

However, using a system containing multiple RGB-D cameras may not be practical due to several problems. First, obviously, additional RGB-D cameras in a 3D reconstruction system will increase the total cost which makes the system less affordable.

Second, simultaneous communication with multiple RGB-D cameras has communication channel bandwidth problems. Therefore, customized hardware is required to capture data from multiple RGB-D cameras simultaneously which is both expensive and requires expert knowledge (Hossny et al., 2012). For example, communicating with more than one Kinect, which is the most popular RGB-D camera among ordinary users, cannot be done on a standard personal computer or laptop on a single USB bus without additional peripherals (Sumar et al., 2011). This is because Kinect contains two separate cameras (RGB and depth cameras) which take all of the available USB bandwidth. Neither USB 2.0 nor 3.0 controllers are capable of supporting more than a single Kinect on a single bus (Sumar et al., 2011). This is a serious limitation that prevents employment

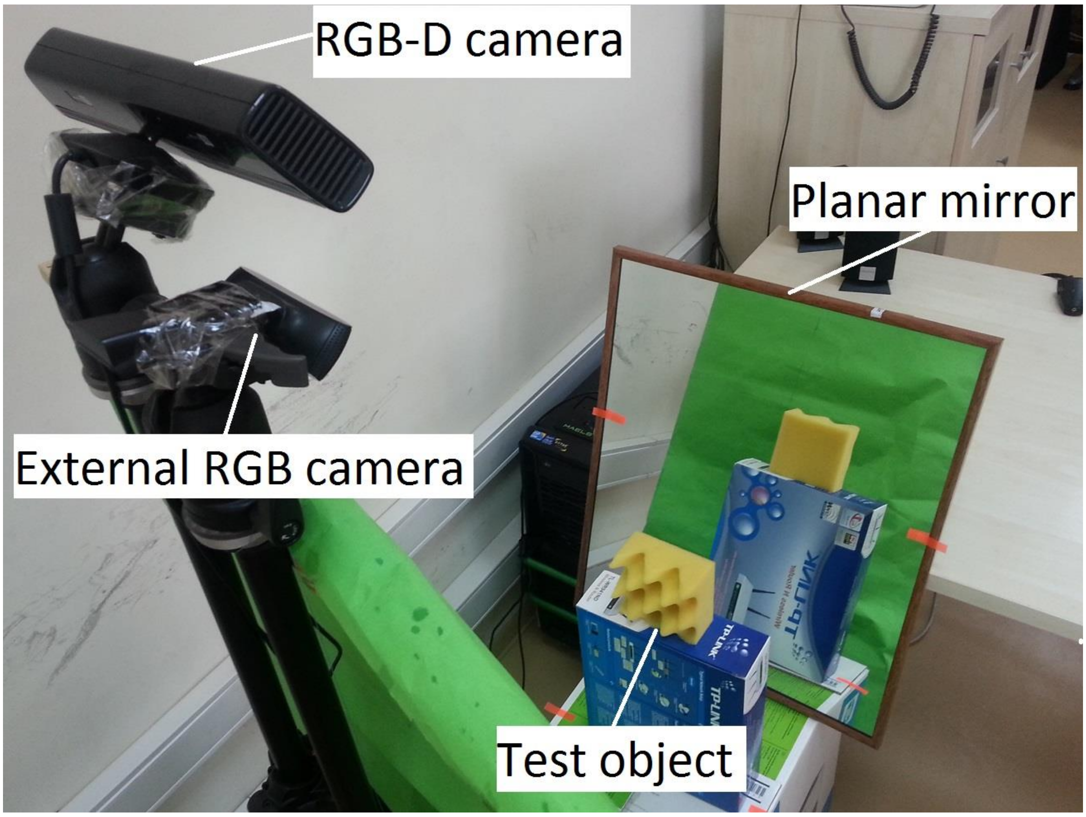

(a)

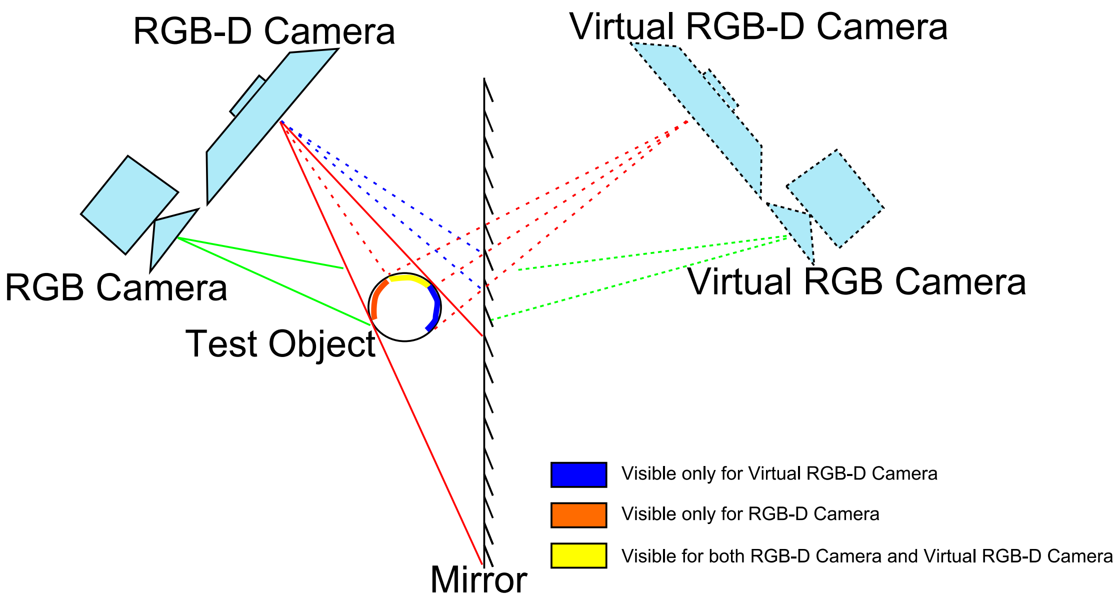

(b)

Figure 1: (a) The test system consists of an RGB-D and an RGB camera observing a test object and its reflection from a planar mirror. (b) Imaging of a round test object with real and virtual RGB-D and RGB cameras.

of multiple Kinects on a standard personal computer. There are additional challenges for multiple RGB-D cameras. Minimum depth sense limitations of the RGB-D cameras is one of these difficulties and there are many applications in which this limitation results in a system failure. For example, reconstructing the 3D structure of a scene is very common for narrow indoor areas such as elevators or industrial production lines. More specifically, in industry, reconstructing the 3D structure of a product or package on a mass production line is crucial for detecting manufacturing defects. Multiple RGB-D cameras can be used to construct the 3D structure of the package and detect defects on it. However, camera minimum depth sense range (50 cm for the Kinect) is quite restrictive for covered production lines and elevators (Canessa et al., 2013; Oliver et al., 2012). In the covered production line case, one can barely fit a single RGB-D camera to inspect products on the conveyor belt. As a result, using multiple cameras for such applications are prohibitive because of the limited space.

Another interesting problem with multiple RGB-D cameras is due to their active sensing technology. All practical RGB-D cameras project infrared or laser light to the scene to estimate the depth values. In the multiple RGB-D camera case, each camera projects its own patterns to the scene. These patterns are accumulated on the overlapped scene surfaces, which causes interference problems among these patterns. This interference adds serious amount of noise to the final depth values (Schröder et al., 2011; Butler et al., 2012).

To overcome the mentioned difficulty, some techniques have been developed. Schröder et al. (2011) proposed a system of synchronized Kinects which enables each Kinect to capture only its own IR dot pattern. They used a fast rotating disk in front of each IR projector so that only one Kinect would project its IR dot pattern to the scene at a given time.

Another interesting solution is Butler et al. (2012). The idea behind the system is to physically vibrate an RGB-D camera using vibration motor. Both IR projector and IR camera of the camera move in harmony which means that depth sensing works as normal with a little blur. However, IR dot patterns of other cameras are sensed blurrily and hence are neglected by other cameras. Therefore each depth camera can sense the depth of the scene almost without noise.

In this paper, we propose a novel method to address the above problems for the 3D reconstruction of a scene using a single or multiple Kinect cameras. We utilize mirrors to create virtual RGB-D cameras so that more views of a scene would be visible from real and virtual RBG-D cameras (Fig.1(a) and Fig. 1(b)). We define the image of the scene from the mirror as a virtual camera image. For example, in Fig. 1(b), the left side of the test object (orange region) can be reconstructed using real RGB-D camera, but the right side of the test object (blue region) is not visible from the real cameras. By placing a mirror behind the test object, we can extract depth data of the blue region which lets us successfully reconstruct 3D structure of the object without additional cameras.

Since each mirror introduces a different view into the system, a more complete 3D reconstruction of the scene can be achieved without any bandwidth, synchronization, cost, and space limitation problems. Our method captures the scene images from the same RGB-D camera, so it uses the same communication channel for real and virtual camera views. This means that our method does not need additional bandwidth for the virtual scene views. Since there is only one RGB-D camera in the system, we do not have any synchronization problems between camera capture times. Adding a planar mirror into the scene is much less expensive than adding more cameras. As a result, our solution is less expensive and it is more practical because adding a planar mirror into the scene can be done by just hanging a mirror on a wall without any need for more depth space. Fig. 2 shows an example configuration for such an application for a covered production line. Note that placing a second RGB-D camera on the location of virtual RGB-D camera is impossible due to minimum depth sense range restrictions.

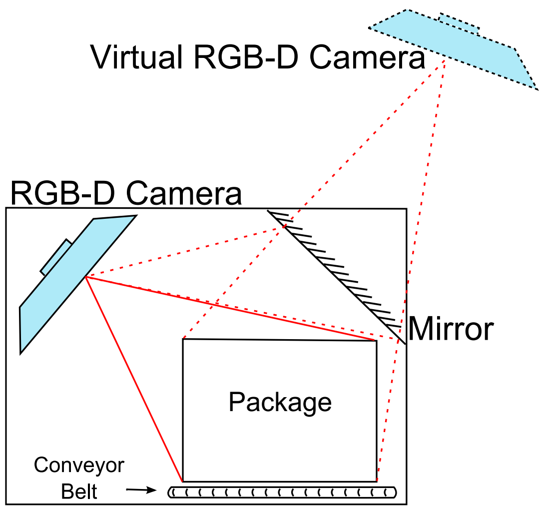

Figure 2: Covered Production Line.

Our method does not address the pattern interference problem, but it can be addressed by

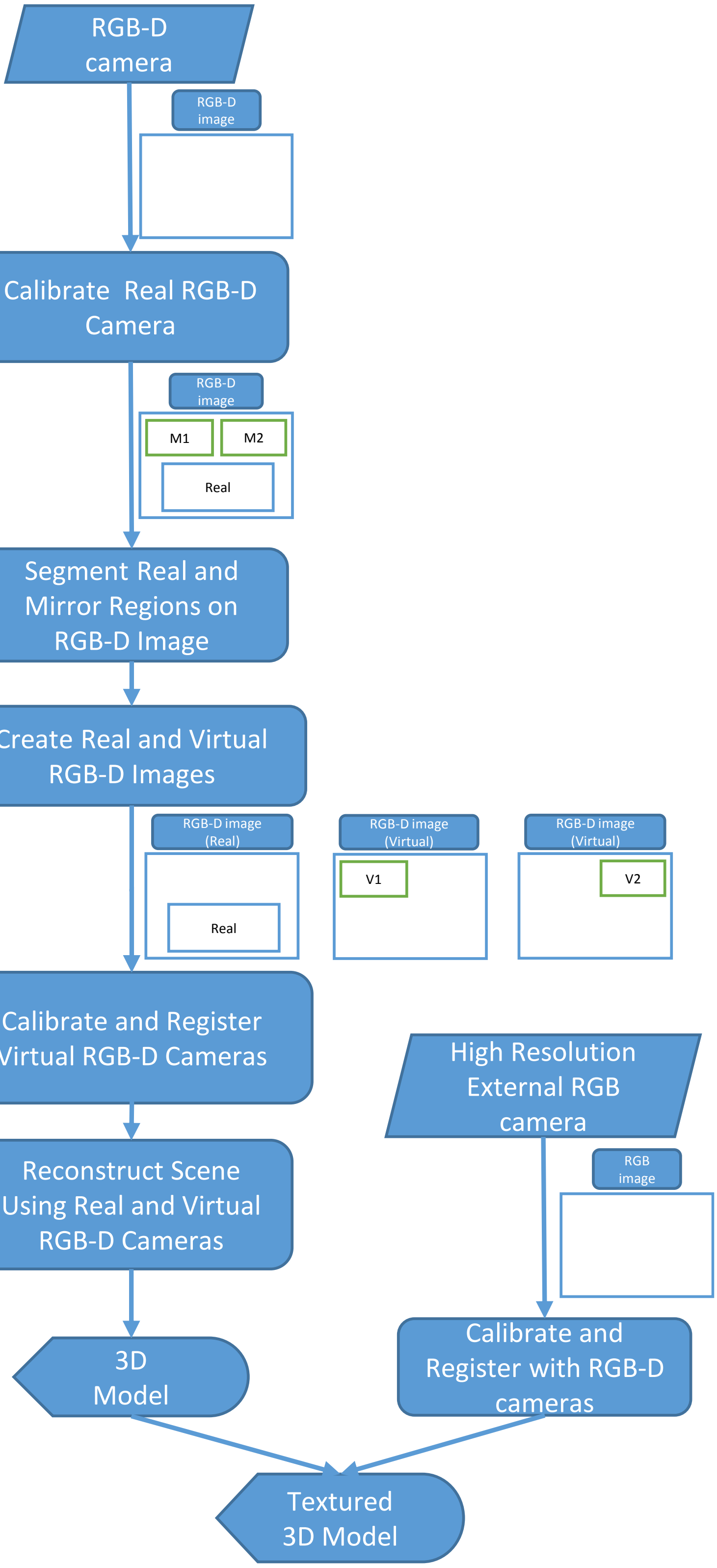

Figure 3: System overview of data flow and main processes

methods introduced by (Schröder et al., 2011; Butler et al., 2012). Finally, our method can also be used with multiple RGB and RGB-D cameras if needed (Fig. 1-b).

There are other work that use mirrors with RGB cameras to reconstruct observed scenes (Nene et al., 1998; Mariottini et al., 2012). They build 3D structure of a scene using Structure from Motion and Stereo techniques. However, these methods are strictly on RGB images and they do not develop any solutions for the problems of RGB-D data such as calibration and registration of depth images.

Using mirrors with RGB-D cameras is not a new idea. There are attempts at using both Kinect and mirrors but these studies are very informal (Kinect vs. Mirror, 2010). They do not develop any algorithms or formulations for the 3D reconstruction of scenes.

Our main contribution in this paper is enabling users to obtain a more complete 3D reconstruction of an object from a single real depth image. Using a proper configuration of mirrors and a single Kinect, one can accomplish 3D reconstruction of an object utilizing proposed method. We develop and test algorithms for the simultaneous calibration and registration of real and virtual RGB-D cameras. We also describe methods for the full 3D reconstruction of the scenes using the developed calibration techniques. Although multiple calibration pattern images with different positions and orientations can be used to calibrate the proposed system, utilizing a single image is found sufficient for the calibration procedure. Furthermore, we used an external high resolution RGB camera to capture high quality images for texture mapping of the reconstructed 3D structure of the object.

The rest of this paper is organized as follows: In Section 2, we give an overview of our method. In Section 3, we describe the calibration/registration procedure between the RGB-D camera and RGB camera. We then explain RGB-D camera - virtual RGB-D camera calibration process. In Section 5, we discuss experimental results of the proposed method. Finally, we provide concluding remarks in Section 6.

2 METHOD OVERVIEW

The main processes and the data flow of the proposed system are shown in Fig. 3. Our systems begins with capturing the RGB-D images of the scene with test or calibration objects. We then calibrate the RGB-D camera using standard calibration procedures. Next, the direct and the reflected image sections of the RGB-D image are segmented as real and virtual RGB-D images, respectively. The calibration and registration of the real and virtual images is followed by the 3D reconstruction of the scene.

RGB-D cameras such as Microsoft's Kinect cannot produce high quality RGB images because of their low resolution and low quality lenses. In order to increase the texture quality of the reconstructed 3D scene, we used an external high resolution RGB camera along with the RGB-D camera (Fig. 1(b)). In other words, we acquire depth data from the RGB-D camera and color data from the external RGB camera. So, we have four cameras in total; two of them are real, two of them are virtual. Calibrating these four cameras enables us to reconstruct the 3D scene with a better texture mapping quality.

3 CALIBRATION AND REGISTRATION

The first step of our method is constructing a test area which is surrounded by single or multiple mirrors. We place a calibration pattern on a location which is visible from both RGB-D camera and external RGB camera (Fig. 4 and Fig. 1(a)). Then, we calibrate intrinsic and extrinsic parameters of the real RGB-D camera and the real RGB camera using the method of Zhang (2000). Next, we perform registration between the RGB-D and the external RGB camera using a method similar to (Jones et al., 2011). Finally, the registration between the real and virtual RGB-D cameras is established. Note that intrinsic parameters of the virtual RGB-D camera and the virtual RGB camera are identical with the real counterparts, which makes the overall calibration of the system easier compared to calibration of multiple real cameras. Next two subsections describe the details of the calibration and the registration processes.

3.1 RGB-D AND RGB CAMERA CALIBRATION

In order to compute the transformation between the real RGB-D camera and the real external RGB camera (Fig. 1(b)), we used the standard calibration pattern (Fig. 4). There are total of 48 calibration corners for a calibration pattern. For a given calibration corner point $C = [X, Y, Z]^T$, the RGB-D camera produces a 3D vector $[x_k, y_k, z_k]^T$ in the camera coordinate space. The image coordinates of

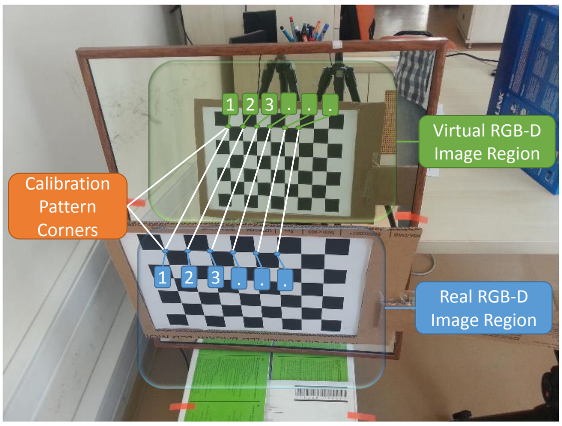

Figure 4: Real and Virtual camera images of the calibration plate. The lines show the correspondence between the real and virtual pattern corners.

the point C on the image plane of the RGB-D camera can be obtained by

$$\left[x_{kp}, y_{kp}, 1\right]^T = \frac{1}{z_k}\left[x_k, y_k, z_k\right]^T, \qquad (1)$$

where $\left[x_{kp}, y_{kp}\right]$ is the image point of C on the RGB-D camera.

We define the intrinsic matrix of the RGB-D camera as,

$$K = \begin{bmatrix} f_x & 0 & c_x \\ 0 & f_y & c_y \\ 0 & 0 & 1 \end{bmatrix}. \qquad (2)$$

The point C is projected on the RGB-D camera's image plane by

$$\begin{bmatrix} x_k \\ y_k \\ z_k \end{bmatrix} = K \begin{bmatrix} X \\ Y \\ Z \end{bmatrix}. \qquad (3)$$

Multiplying both sides with K^{-1} will lead,

$$K^{-1}\begin{bmatrix} x_k \\ y_k \\ z_k \end{bmatrix} = \begin{bmatrix} X \\ Y \\ Z \end{bmatrix}. \qquad (4)$$

We multiply both sides with $\frac{1}{z_k}$ then the equation becomes,

$$K^{-1}\begin{bmatrix} x_{kp} \\ y_{kp} \\ 1 \end{bmatrix} = \begin{bmatrix} X/z_k \\ Y/z_k \\ Z/z_k \end{bmatrix}. \qquad (5)$$

Using the above equation, one can reconstruct the scene whose depth data is acquired from RGB-D camera.

Since we know K^{-1} and $\begin{bmatrix} x_{kp} \\ y_{kp} \\ 1 \end{bmatrix}$, we can compute $[X/z_k \quad Y/z_k \quad Z/z_k]^T$.

Moreover, as Z_k is already known from the RGB-D depth data, the scale factor z_k is easily extracted which enables us to compute $[X, Y, Z]^T$.

Let $\left[x_r, y_r\right]^T$ be the image of point C on the RGB camera. At this point, we have a set of $[X, Y, Z]^T$ and $\left[x_r, y_r\right]^T$ correspondences which is required to compute projection matrix between the real world coordinates and the RGB camera. We compute this projection matrix using the Singular Value Decomposition (SVD) method.

3.2 RGB-D AND VIRTUAL RGB-D CAMERA CALIBRATION

In order to compute the transformation between the real and virtual RGB-D cameras (Fig. 1(b)), we used a two-sided calibration pattern whose corners are projections of the same 3D point for all cameras (Fig. 4).

Without loss of generality, we assume that the camera reference frame of the real RGB-D camera is the same as the world reference frame. Let $[X, Y, Z]^T$ be the coordinate of the calibration pattern corner C in RGB-D camera reference frame. Let $[X_v, Y_v, Z_v]^T$ be the coordinate of C in virtual RGB-D camera reference frame. We can compute $[X_v, Y_v, Z_v]^T$ with the method mentioned in the previous subsection (Eq. 5).

$C = [X, Y, Z]^T$ and $C_v = [X_v, Y_v, Z_v]^T$ vectors refer to the same calibration pattern corner in different reference frames; real and virtual RGB-D camera reference frames, respectively. This is because we used a two-sided calibration pattern to capture the calibration points (Fig. 5). Hence the transformation between the reference frames of the RGB-D and the virtual RGB-D camera can be computed utilizing these correspondences.

We follow the procedure described by (Besl et al., 1992) to calculate the rotation matrix and the

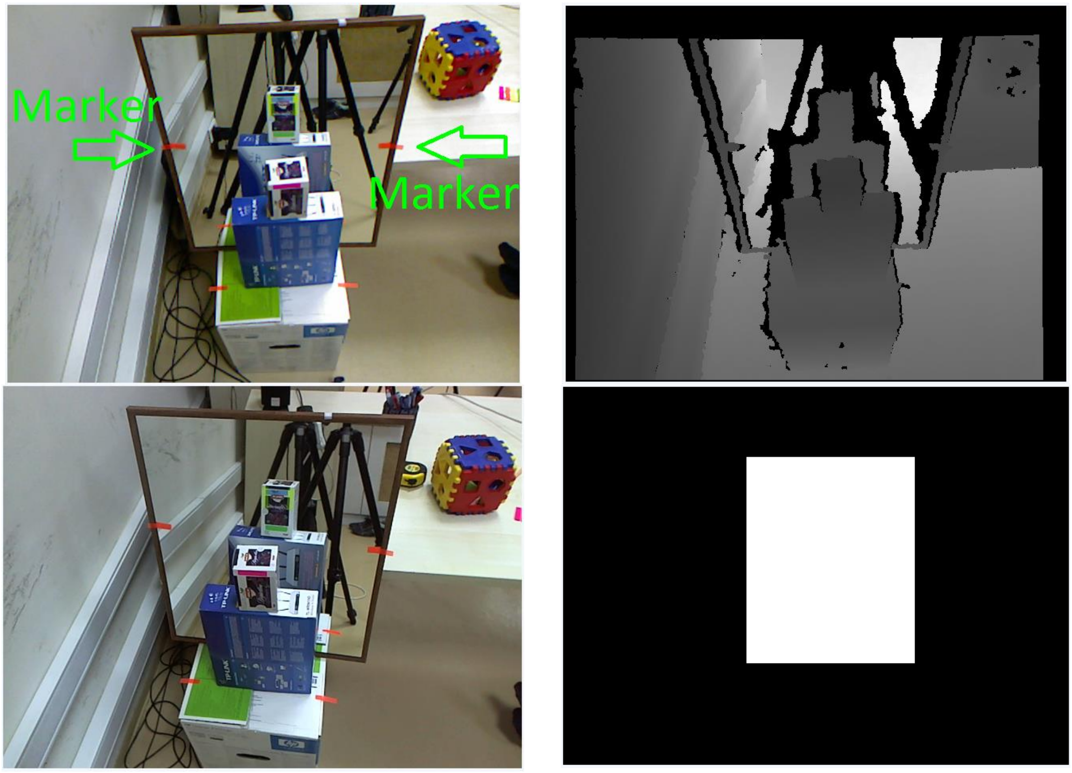

Figure 5: RGB-D camera's RGB image (top-left), RGB-D camera's depth image (top-right), external RGB image (bottom-left) and current workspace mask (bottom-right).

translation vector between the reference frames of real and virtual RGB-D cameras. Let Cen be the centroid of the corners points of the RGB-D camera. Similarly, let Cen_v be the centroid of the corner points of the virtual RGB-D camera.

$$\begin{aligned} Cen &= \frac{1}{N}\sum_{i=1}^{N} C^i. \\ Cen_v &= \frac{1}{N}\sum_{i=1}^{N} C_v^i. \end{aligned} \qquad (6)$$

Where C^i and C_v^i are the i^{th} corner points of the real and virtual cameras, respectively. N is the number of points in the point set.

We accumulate point-centroid distances in the 3x3 matrix H,

$$H = \sum_{i=1}^{N}\left(C^i - Cen\right) . \left(C_v^i - Cen_v \right)^T, \qquad (7)$$

where . represents matrix multiplication. By decomposing H using SVD we obtain,

$$[U,S,V] = SVD(H). \qquad (8)$$

The rotation matrix R can be computed as,

$$R = VU^T, \qquad (9)$$

and translation vector T can be computed using,

$$T = -R\ Cen + Cen_v. \qquad (10)$$

Now, we have R and T between RGB-D and virtual RGB-D camera reference frames. To transform a 3D point from the RGB-D camera reference frame to the virtual RGB-D camera reference frame, following formula can be used

$$C_v = RC + T. \qquad (11)$$

4 RECONSTRUCTION

In the 3D reconstruction phase, we first acquire the depth image from the RGB-D camera. RGB images are obtained from both RGB-D and external RGB cameras. In order to determine which regions of images belong to the real scene and which belong to the virtual scene (mirror regions), we place markers on the borders of the mirror frame (Fig. 5). We locate marker positions on the RGB image of the RGB-D camera. As we have already registered the depth and the RGB cameras of the RGB-D camera, we can transform pixel coordinates of the markers from RGB image reference frame to depth image reference frame. Then, we get the depth value of the markers. The surface points whose depth values are lower than marker's depth value are assumed to belong to the real scene and others are assumed to belong to the virtual scene, which are actually reflections of the real objects on the mirror. After separating real and virtual surface points, we reconstruct the real surface points using eq. (5) and build a point cloud with these points. We achieve reconstruction of virtual surface points via the same technique that we use for the real surfaces. Next, we transform the reconstructed virtual surface points from the virtual RGB-D camera reference frame to the real RGB-D camera reference frame using Eq.11. Finally, we merge the transformed virtual surface points with the point cloud constructed using the real surface points. Overlapped regions which are visible from both real and virtual RGB-D cameras are not specially treated, which means that for some object sections, there might be more than one 3D reconstruction point. After the reconstruction, we find the color value of each 3D point using the method described in section 3.1.

Table 1: Calibration and reconstruction results

	Avg Err	Std Dev
Ext. Cam. - Real RGB-D camera	1.68 px	1.21 px
Real - Virtual RGB-D camera	5.00 mm	2.39 mm
Real - Reconstructed distance	4.21 mm	3.05 mm

5 EXPERIMENTAL RESULTS

In order to show quantitative results of our method we conducted some experiments. We reconstructed 3D points that correspond to calibration plate corners and projected these points onto the RGB camera image plane to measure the external RGB and RGB-D camera calibration error (Fig. 4). The average distance between the projected 3D points and detected corner pixels (Ground truth) is presented in the first row of Table 1 with standard deviation. Next, we repeated the same experiment between the real and virtual RGB-D cameras. We reconstructed two sets of 3D points using the calibration plate corners from the real RGB-D camera and the virtual RGB-D camera. Then, we transform set of virtual 3D points from the virtual RGB-D camera reference frame to the real RGB-D camera reference frame to calculate the transformation error. The second row of Table 1 contains the average distance between the transformed 3D points and the ground truth 3D points and its standard deviation.

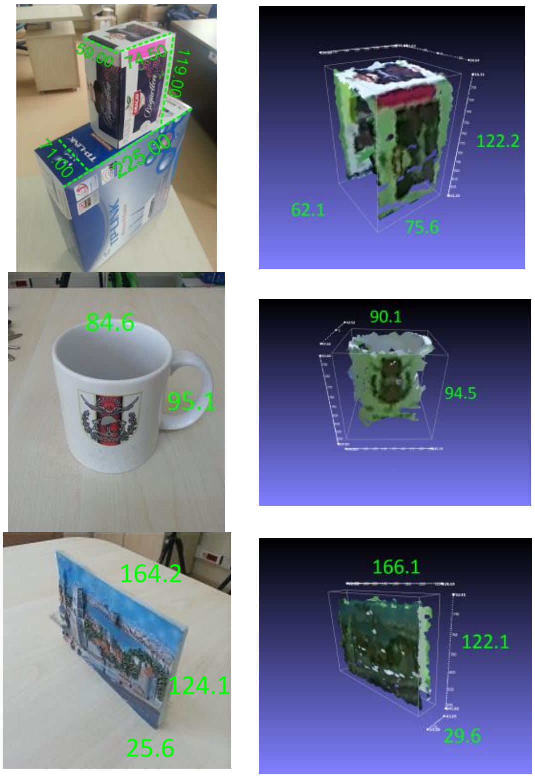

Figure 6: Ground truth measurements (mm) of the test object (left), Distances measured by our method (right)

Finally, we compare reconstructed object size measurements with the ground truth object size measurements. The ground truth object size measurements were obtained by using a standard caliper tool on the real world objects. The last row of Table 1 shows the average difference between the reconstructed distances and the ground truth distances with standard deviation. Fig. 6 shows some of the test objects used to assess our system. Note that, without using our virtual RGB-D camera setup, these types of measurements are very difficult to obtain from a single depth map image.

We also provide qualitative results for some 3D reconstruction examples in Fig. 7. Left column represents RGB image of the objects, middle column and right column represent frontal and rear view of reconstructed 3D objects, respectively.

6 CONCLUSIONS

The availability of the RGB-D cameras made the 3D reconstruction tasks much easier compared to earlier systems. Using multiple RGB-D cameras are now becoming more popular for a more complete 3D reconstruction. We presented a new method that uses RGB-D cameras with mirrors to prevent a number of known problems such as synchronization, physical space limitations, bandwidth limitations, and inherent costs. We provided formulations for the calibration and registration of multiple real and virtual RGB-D and RGB cameras. We also provided formulations for the reconstruction task from the obtained data. Our method is capable of producing reconstruction results with higher texture quality by employing an external high resolution RGB camera. One drawback of our method is that, the real and virtual cameras have to share the same image space which introduces a resolution problem. In addition, the depth noise from virtual RGB-D camera will increase due to the increased distance. However, this problem will be less important as higher resolution RGB-D cameras become available. The experiments performed on real test objects showed qualitatively and quantitatively that our method is very effective in practice.

ACKNOWLEDGEMENTS

This work is supported by TUBITAK Project 112E127.

REFERENCES

1. Smisek, Jan, Michal Jancosek, and Tomas Pajdla. "3D with Kinect." *Consumer Depth Cameras for Computer Vision*. Springer London, 2013. 3-25.
2. Henry, Peter, et al. "RGB-D mapping: Using Kinect-style depth cameras for dense 3D modeling of indoor environments." *The International Journal of Robotics Research* 31.5 (2012): 647-663.
3. Khoshelham, Kourosh, and Sander Oude Elberink. "Accuracy and resolution of kinect depth data for indoor mapping applications." *Sensors* 12.2 (2012): 1437-1454.
4. Izadi, Shahram, et al. "KinectFusion: real-time 3D reconstruction and interaction using a moving depth camera." *Proceedings of the 24th annual ACM symposium on User interface software and technology*. ACM, 2011.
5. Rusu, Radu Bogdan, and Steve Cousins. "3d is here: Point cloud library (pcl)."*Robotics and Automation (ICRA), 2011 IEEE International Conference on*. IEEE, 2011.
6. Canessa, Andrea, et al. "Calibrated depth and color cameras for accurate 3D interaction in a stereoscopic augmented reality environment." *Journal of Visual Communication and Image Representation* (2013).
7. Oliver, Ayrton, et al. "Using the Kinect as a navigation sensor for mobile robotics." *Proceedings of the 27th Conference on Image and Vision Computing New Zealand*. ACM, 2012.
8. Lai, Kevin, et al. "A large-scale hierarchical multi-view rgb-d object dataset."*Robotics and Automation (ICRA), 2011 IEEE International Conference on*. IEEE, 2011.
9. Sumar, Lazar, and Andrew Bainbridge-Smith. "Feasibility of Fast Image Processing Using Multiple Kinect Cameras on a Portable Platform." *Department of Electrical and Computer Engineering, Univ. Canterbury, New Zealand.*
10. Hossny, M., et al. "Low cost multimodal facial recognition via kinect sensors."*LWC 2012: Potent land force for a joint maritime strategy: Proceedings of the 2012 Land Warfare Conference*. Commonwealth of Australia.
11. Schröder, Y., Scholz, A., Berger, K., Ruhl, K., Guthe, S., & Magnor, M. (2011). Multiple kinect studies. *Computer Graphics*.
12. Butler, D. Alex, et al. "Shake'n'sense: reducing interference for overlapping structured light depth cameras." *Proceedings of the 2012 ACM annual conference on Human Factors in Computing Systems*. ACM, 2012.
13. Nene, Sameer A., and Shree K. Nayar. "Stereo with mirrors." *Computer Vision, 1998. Sixth International Conference on*. IEEE, 1998.
14. Mariottini, Gian Luca, et al. "Planar mirrors for image-based robot localization and 3-D reconstruction." *Mechatronics* 22.4 (2012): 398-409.
15. "Kinect vs. Mirror," http://www.youtube.com/watch?v=1Qx8NzuSSJ4
16. Zhang, Z. 2000. A flexible new technique for camera calibration. IEEE TPAMI, 22(11):1330–1334.
17. Jones, Brett R. *Augmenting Complex Surfaces With Projector-Camera Systems*. Diss. University of Illinois, 2011.
18. Besl, Paul J., and Neil D. McKay. "Method for registration of 3-D shapes." *Robotics-DL tentative. International Society for Optics and Photonics*, 1992.

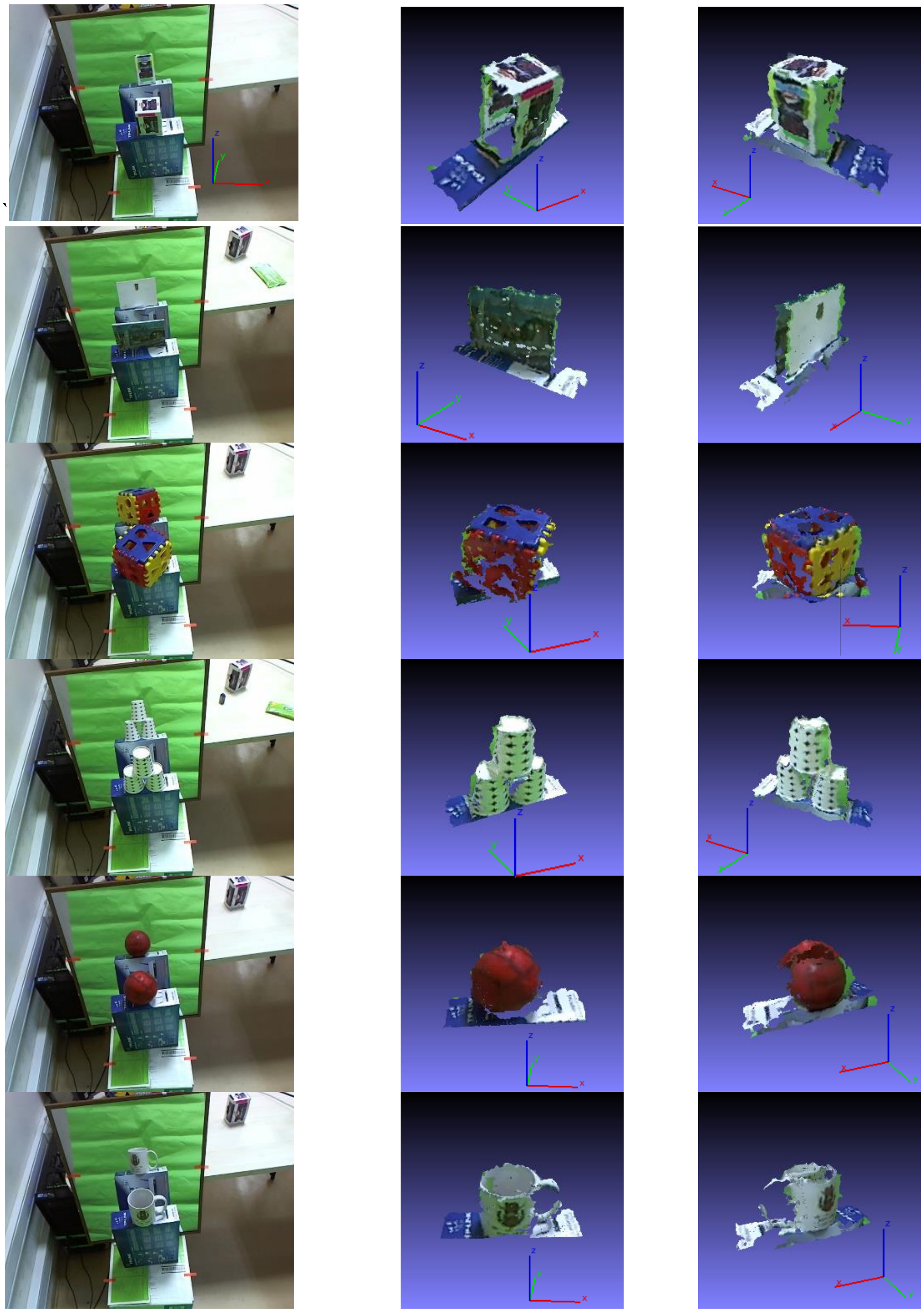

Figure 7: Reconstruction results